

Study of Higgs \rightarrow invisible using kinematic fit method applied jet energy resolution of ILD

Yu Kato, J.Tian, T.Tanabe, S.Yamashita
The Univ. of Tokyo

Outline

- ❑ Motivation

- ❑ Idea for improvement

- ❑ Flow of study

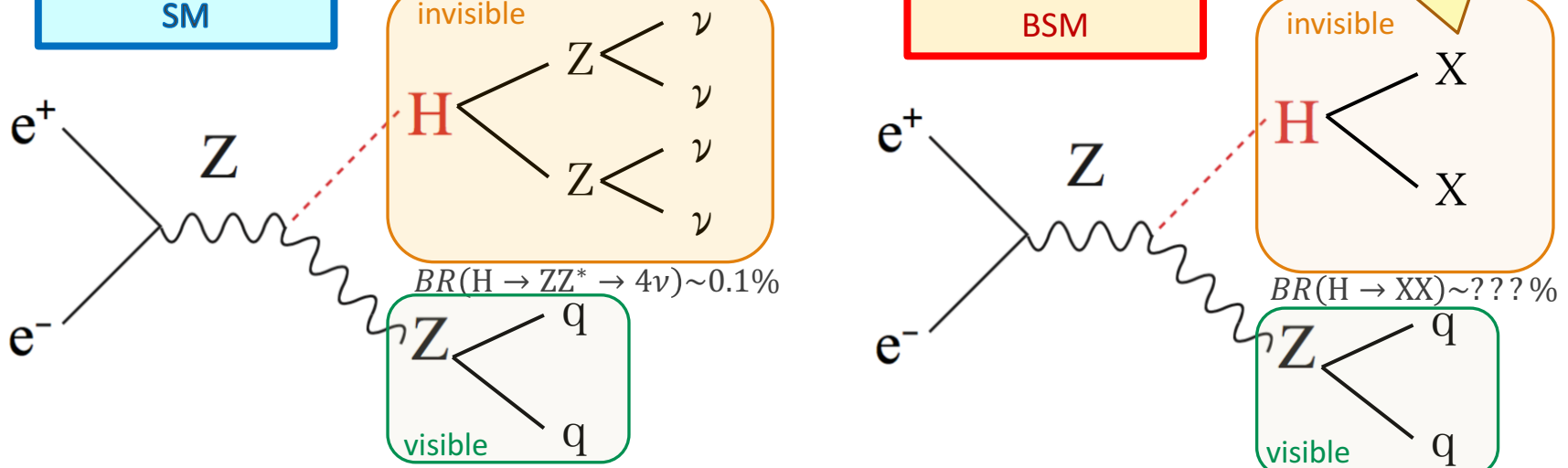
- ◆ Evaluate jet energy resolution
- ◆ kinematic fit
- ◆ Analysis Higgs→invisible

- ❑ Summary & Plans

Motivation

- In SM, Higgs decays invisibly through $H \rightarrow ZZ^* \rightarrow 4\nu$ ($BR(H \rightarrow inv.) \sim 0.1\%$)
- If $BR(H \rightarrow inv.)$ exceeds SM prediction , it signifies new physics beyond SM (BSM)
- We estimate SM upper limit of $BR(H \rightarrow inv.)$
- Compare result between left & right polarization

Previous study (A.Ishikawa)
(95% CL, 250fb^{-1})
left pol. : right pol.
0.95% : 0.69%



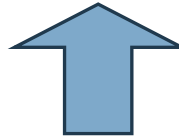
➤ A. Ishikawa (Tohoku Univ.),
"Search for Invisible Higgs Decays at the ILC" LCWS2014@Belgrade

Idea for improvement

Improve analysis performance



kinematic fit



apply jet energy resolution

Flow of study

Evaluate jet energy resolution

ILD model : ILD_I(s)5_v02

➤ jet energy & $\cos \theta$ dependence

evaluate jet angle resolution also → apply to kinematic fit

kinematic fit

fit variables : $E_{j1}, \theta_{j1}, \phi_{j1}, E_{j2}, \theta_{j2}, \phi_{j2}$

constraint : $m_{jj} = m_Z = 91.2 \text{ GeV}$

use MarlinKinfit - fitter engine : OPALFitter

apply jet resolution

➤ check effect & accuracy of fit

Improve analysis performance

[BSM search using Higgs→invisible]

Evaluate jet energy resolution

Setting of Evaluation JER

- ILCSoft : v01-19-05 (gcc49)
- ILDConfig : v01-19-05-p01
- ILD models : ILD_I5_o1_v02, (ILD_s5_o1_v02)
- samples : $Z \rightarrow uds$ (w/o overlay)

\sqrt{s} [GeV]	30	40	60	91	120	160	200	240	300	350	400	500
I5 [events]	10k	9k	10k	9k	10k							
s5 [events]	10k	10k	10k	10k	9k	10k	10k	9k	10k	10k	10k	10k

- jet resolution definition
 - use RMS₉₀ method
 - Energy

$$\frac{\sigma_E}{E} = \frac{\text{RMS}_{90}(E_j)}{\text{mean}_{90}(E_j)} = \sqrt{2} \frac{\text{RMS}_{90}(E_{jj})}{\text{mean}_{90}(E_{jj})}$$

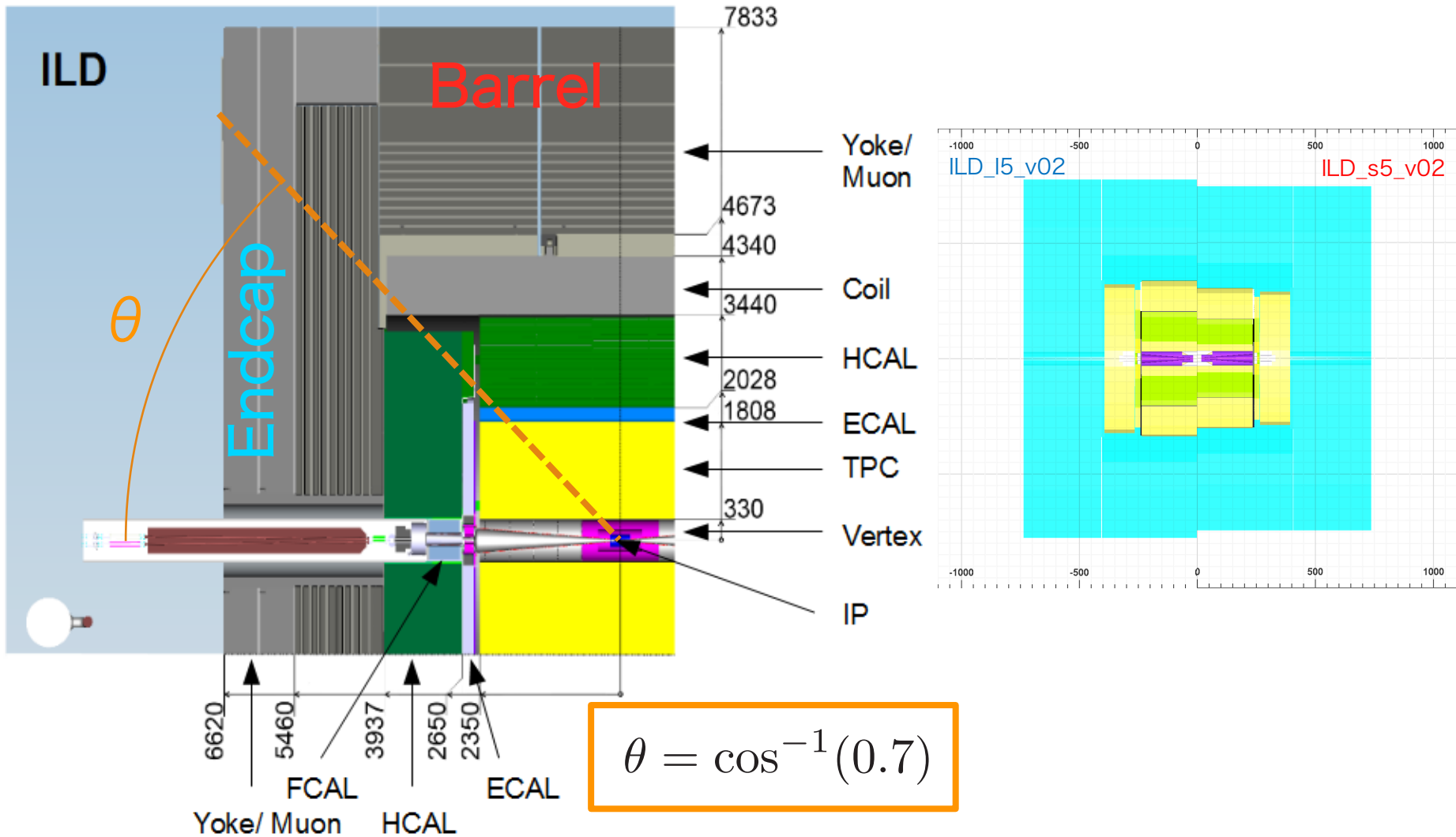
(J. S. Marshall and M. A. Thomson, "Pandora Particle Flow Algorithm", [arXiv:1308.4537](https://arxiv.org/abs/1308.4537) [physics.ins-det])

- Angle use jet clustering: Durham

$$\delta\phi = \text{RMS}_{90}(\phi_{rec} - \phi_{mc})$$

$$\delta\theta = \text{RMS}_{90}(\theta_{rec} - \theta_{mc})$$

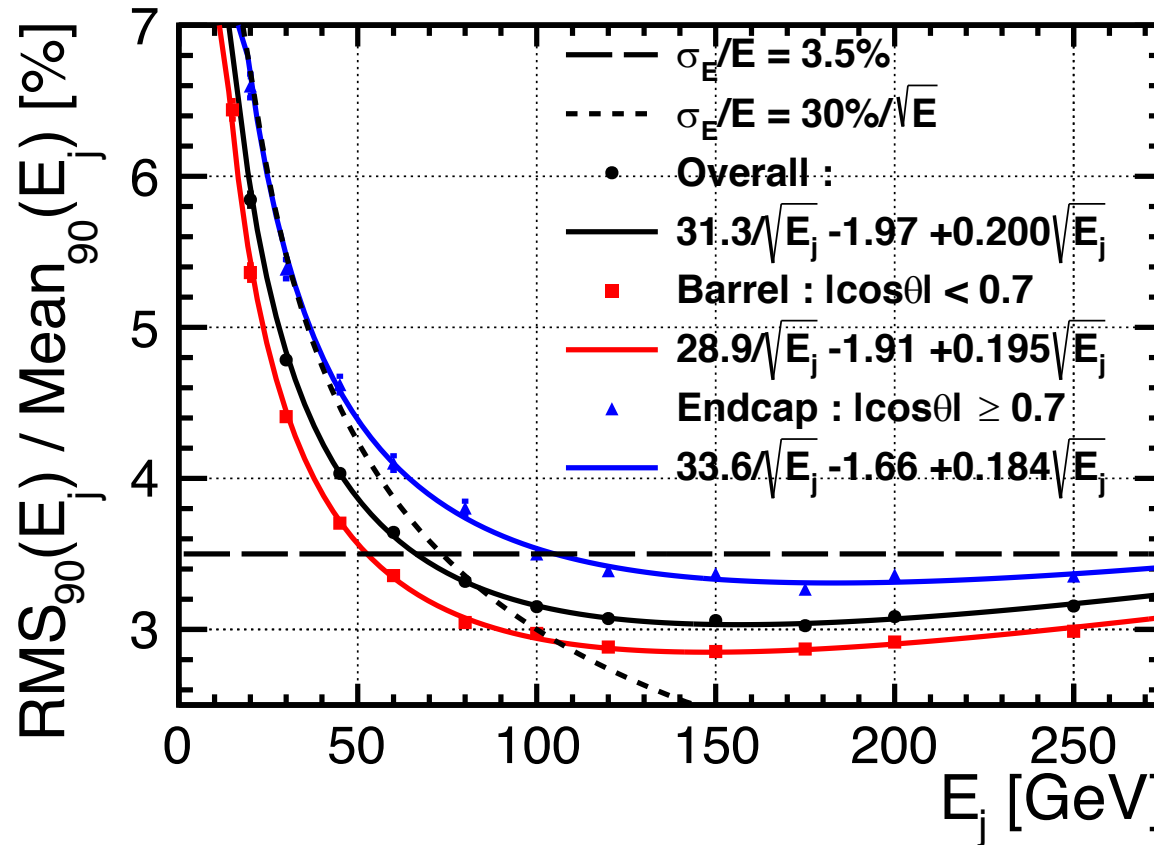
ILD model Detailed Baseline Design



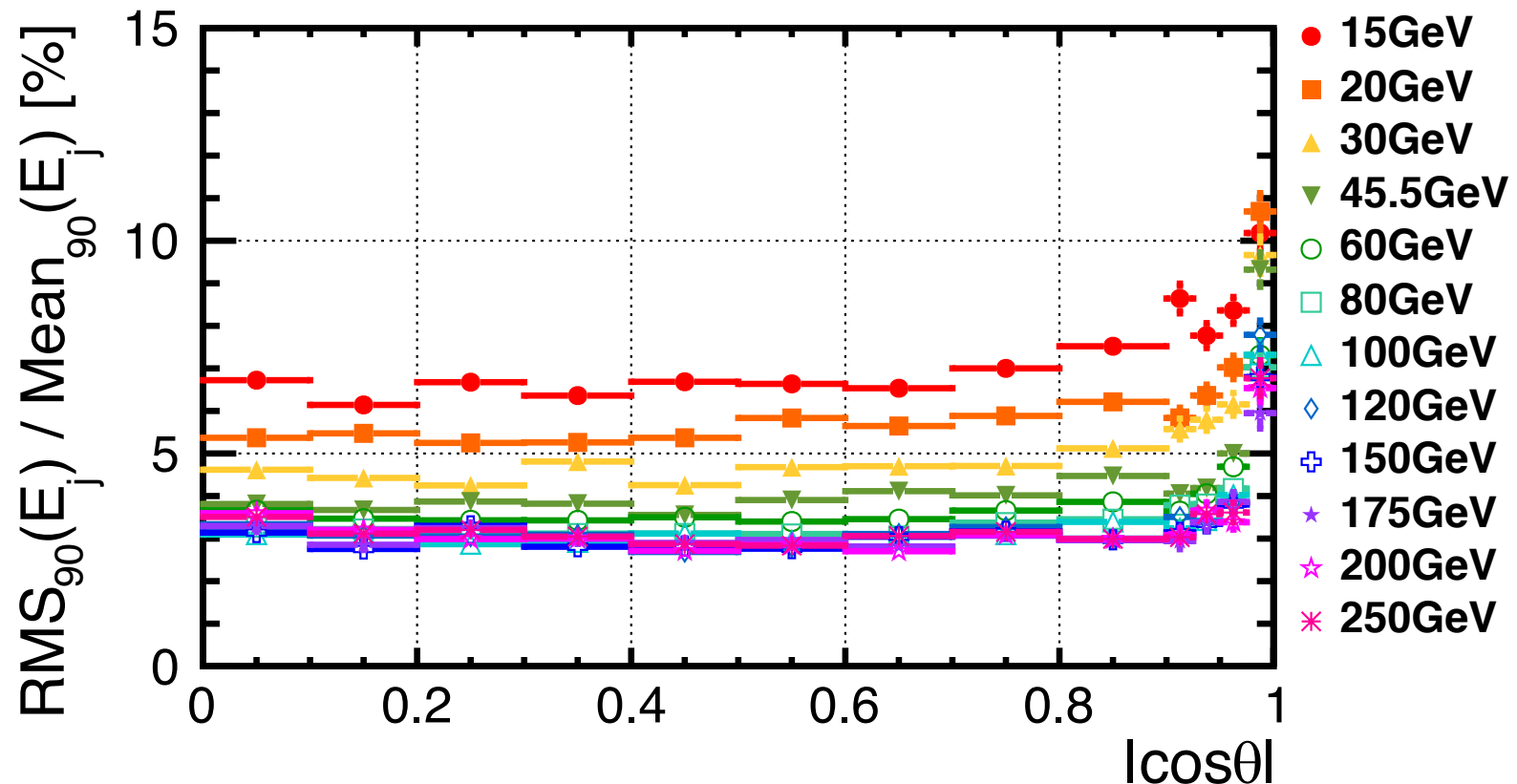
Result : Energy dependence

$$\frac{\sigma_E}{E} = \frac{\alpha}{\sqrt{E}} \oplus \beta(E)$$

sv01-19-05.mILD_I5_o1_v02_nobg



Result : energy & angle dependence

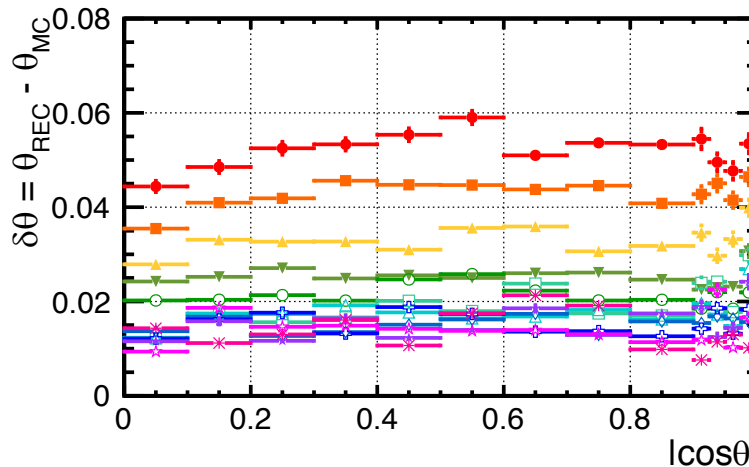
sv01-19-05.mILD_I5_o1_v02_nobg**apply this result to kinematic fit**

Angular resolution

polar angle

$$\delta\theta = RMS_{90}(\theta_{rec} - \theta_{mc})$$

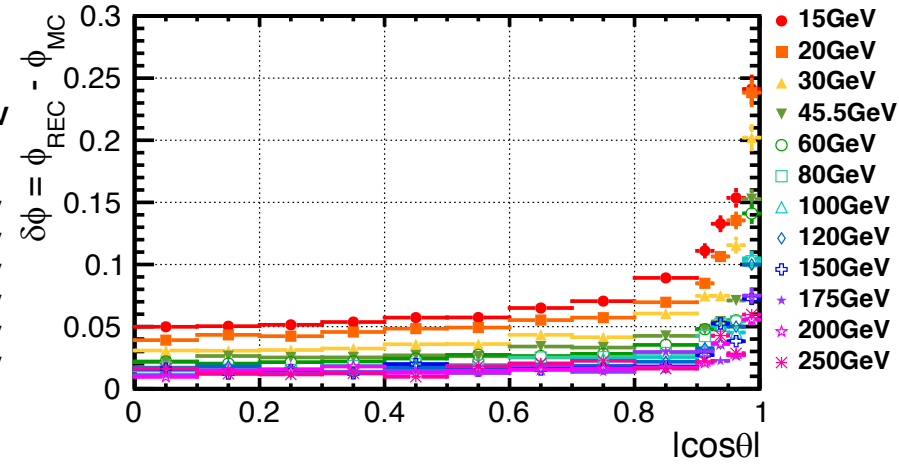
sv01-19-05.mILD_I5_o1_v02_nobg



azimuth angle

$$\delta\phi = RMS_{90}(\phi_{rec} - \phi_{mc})$$

v01-19-05.mILD_I5_o1_v02_nobg



For evaluation of angular resolution,
use jet clustering.

Durham algorithm

$$y_{ij} = \frac{2\min(E_i^2, E_j^2)(1 - \cos\theta_{ij})}{Q^2}$$

apply this result to kinematic fit

kinematic fit

Principle of kinematic fit

seek minimum of $\chi_T^2(\vec{\eta}, \vec{\xi}, \vec{\lambda})$
under kinematic constraints

$$\chi_T^2(\vec{\eta}, \vec{\xi}, \vec{\lambda}) = \chi^2(\vec{\eta}) + F_C(\vec{\eta}, \vec{\xi}, \vec{\lambda})$$

$$\chi^2(\vec{\eta}) = (\vec{\eta} - \vec{y})^T V^{-1} (\vec{\eta} - \vec{y})$$

$$F_C(\vec{\eta}, \vec{\xi}, \vec{\lambda}) = 2\vec{\lambda}^T \cdot \vec{f}(\vec{\eta}, \vec{\xi})$$

method of Lagrange multipliers

$$\left\{ \begin{array}{l} \frac{1}{2} \frac{\partial \chi_T^2}{\partial \eta_i} = V_{ij}^{-1} (\eta_j - y_j) + \frac{\partial f_k}{\partial \eta_i} \lambda_k = 0 \quad (i = 1, \dots, N) \\ \frac{1}{2} \frac{\partial \chi_T^2}{\partial \xi_i} = \frac{\partial f_k}{\partial \xi_i} \lambda_k = 0 \quad (i = 1, \dots, J) \\ \frac{1}{2} \frac{\partial \chi_T^2}{\partial \lambda_i} = f_i = 0 \quad (i = 1, \dots, K) \end{array} \right.$$

$$\text{d.o.f. : } N_{dof} = N_m - \{N_f - (K - J)\} = K - J$$

\vec{y} : measured values (N)

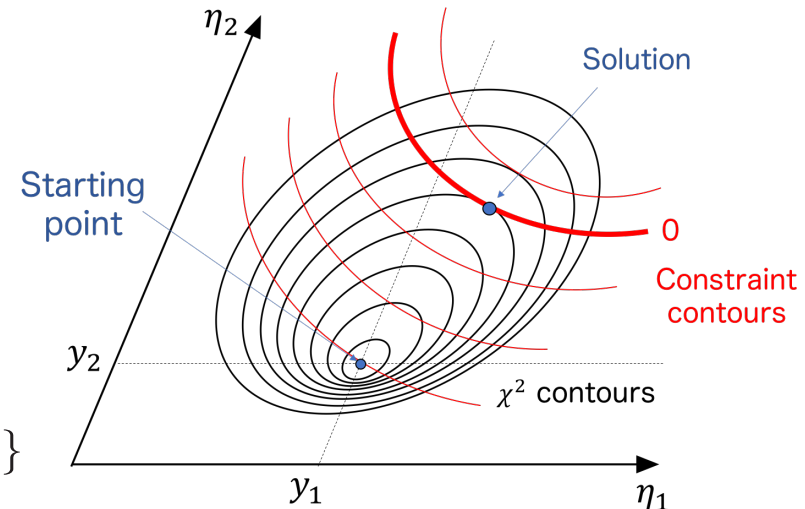
$\vec{\eta}$: fit parameters (N)

$\vec{\xi}$: unmeasured parameters (J)

$\vec{\lambda}$: Lagrange multipliers (K)

\vec{f} : constraint functions (K)

V : covariance matrix ($N \times N$)

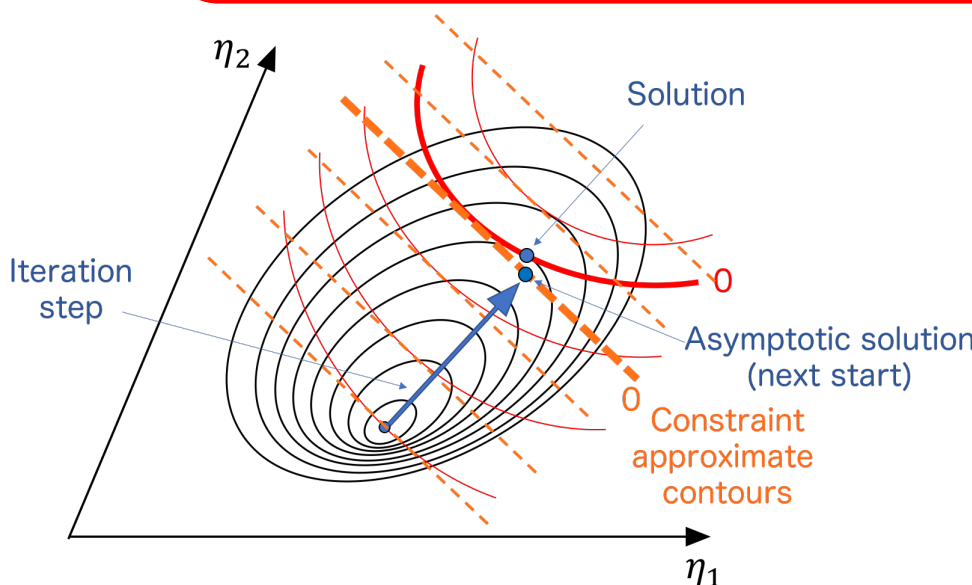


MarlinKinfit : OPALFitter

For iterative solution : Taylor-expansion of the constraints

$$f_i(\vec{\eta}^{\nu+1}, \vec{\xi}^{\nu+1}) = f_i(\vec{\eta}^\nu, \vec{\xi}^\nu) + \frac{\partial f_i}{\partial \eta_j} \Big|_{\eta_j=\eta_j^\nu} (\eta_j^{\nu+1} - \eta_j^\nu) + \frac{\partial f_i}{\partial \xi_k} \Big|_{\xi_k=\xi_k^\nu} (\xi_k^{\nu+1} - \xi_k^\nu)$$

$$\left\{ \begin{array}{l} V_{ij}^{-1}(\eta_j^{\nu+1} - y_j) + \frac{\partial f_k}{\partial \eta_i} \Big|_{\eta_i=\eta_i^\nu} \lambda_k^{\nu+1} = 0 \quad (i = 1, \dots, N) \\ \frac{\partial f_k}{\partial \xi_i} \Big|_{\xi_i=\xi_i^\nu} \lambda_k^{\nu+1} = 0 \quad (i = 1, \dots, J) \\ f_i(\vec{\eta}^{\nu+1}, \vec{\xi}^{\nu+1}) = 0 \quad (i = 1, \dots, K) \end{array} \right.$$

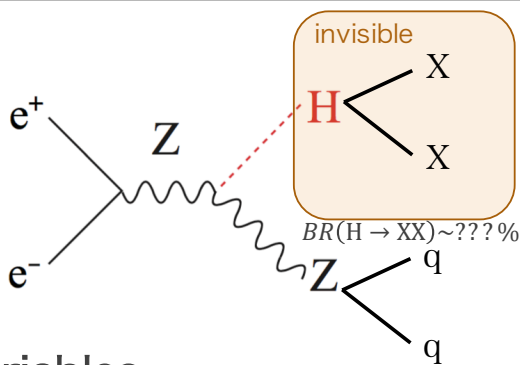


Convergence condition

- ✓ $\delta\chi^2 < 0.01\% \cap \delta F_C < 10^{-3}$
 $\cap F_C < 10^{-2} \cdot \chi^2$
- or
- ✓ all $f_i < 10^{-6} \cap \delta(\eta, \xi, \lambda) < 10^{-6}$

kinematic fit

ZH processor



Fit variables

$$E_{j1}, \theta_{j1}, \phi_{j1}, E_{j2}, \theta_{j2}, \phi_{j2}$$

Z mass constraint

$$m_{jj} = m_Z = 91.2 \text{ GeV}$$

jet mass constraint

$$m_j^{\text{before}} = m_j^{\text{after}}$$

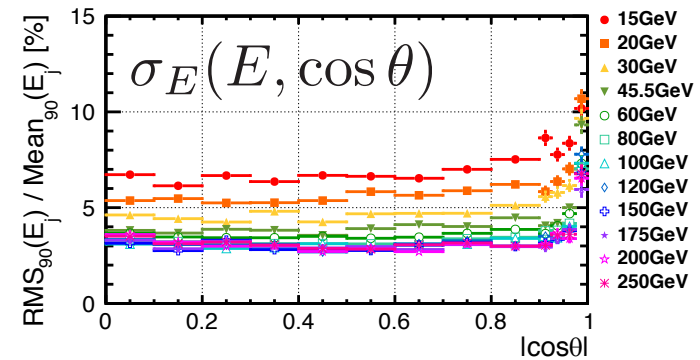
Implement of jet resolution

$$\sigma_E(E, \cos \theta), \sigma_\theta(E, \cos \theta), \sigma_\phi(E, \cos \theta)$$

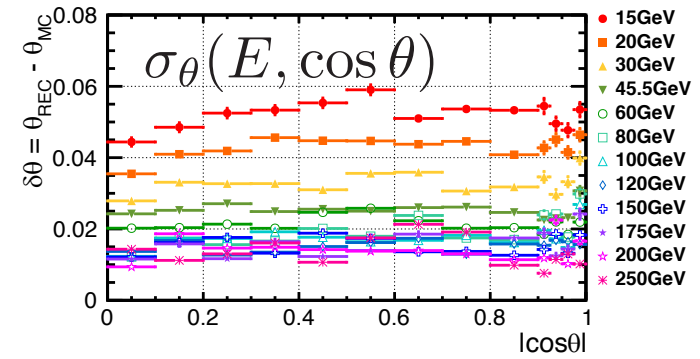
degrees of freedom

$$\begin{aligned} N_{\text{dof}} &= N_m - \{N_f - (K - J)\} \\ &= K - J = 1 \end{aligned}$$

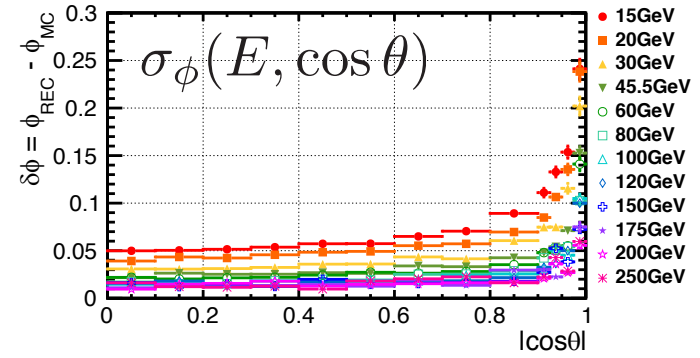
sv01-19-05.mILD_l5_o1_v02_nobg



sv01-19-05.mILD_l5_o1_v02_nobg

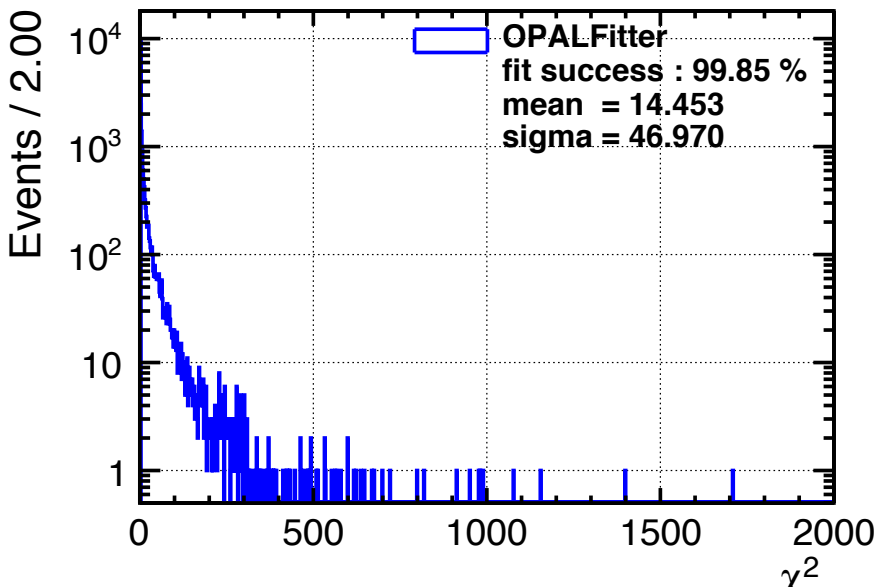


sv01-19-05.mILD_l5_o1_v02_nobg



Result : accuracy of fit

sv01-19-05.mILD_o1_v05.eL.pR



χ^2 distribution

Mean : 14.5

Ndof : 1

Mean > Ndof

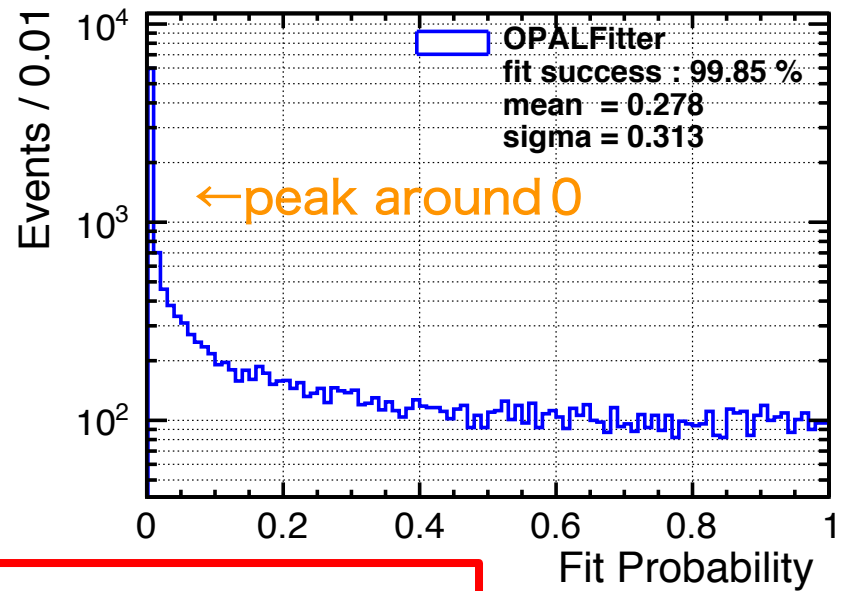
fit probability

$$= \int_{\chi^2_{result}}^{\infty} f_{\chi^2}(\chi^2; \nu) d\chi^2$$

fit with well-estimated errors

→ normal distributed between 0 and 1

sv01-19-05.mILD_o1_v05.eL.pR



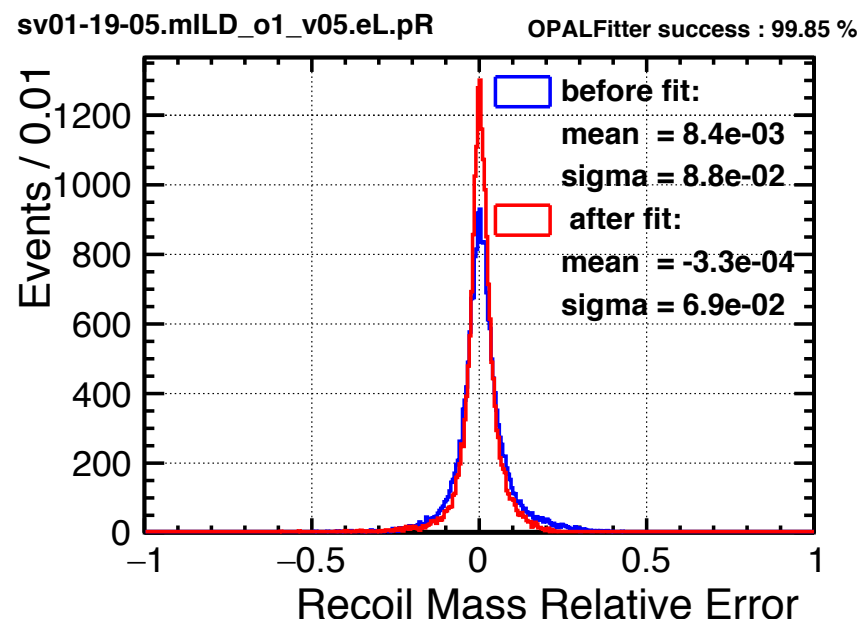
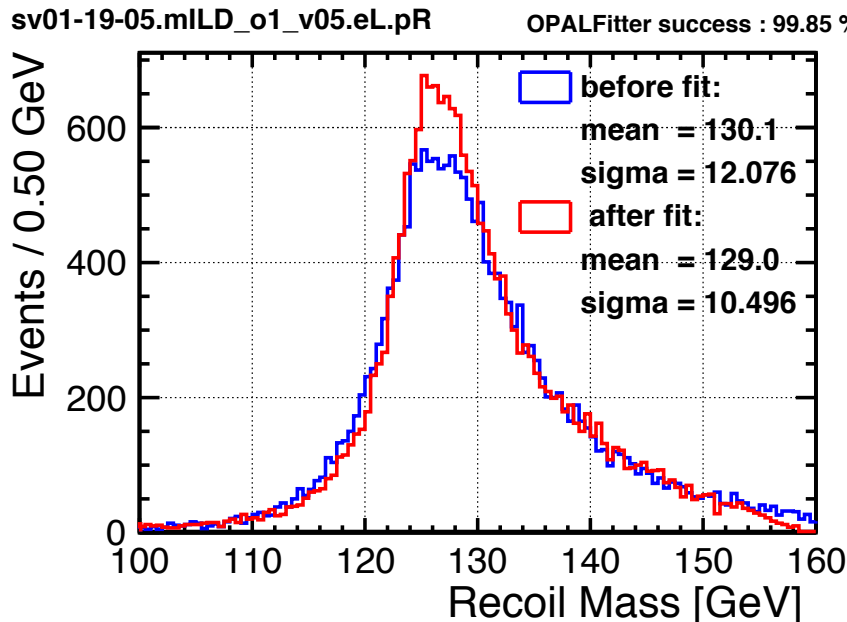
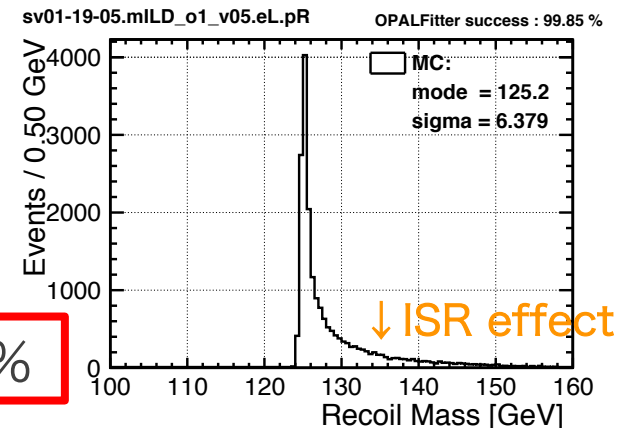
a possibility of underestimating parameter error

Result : Recoil mass

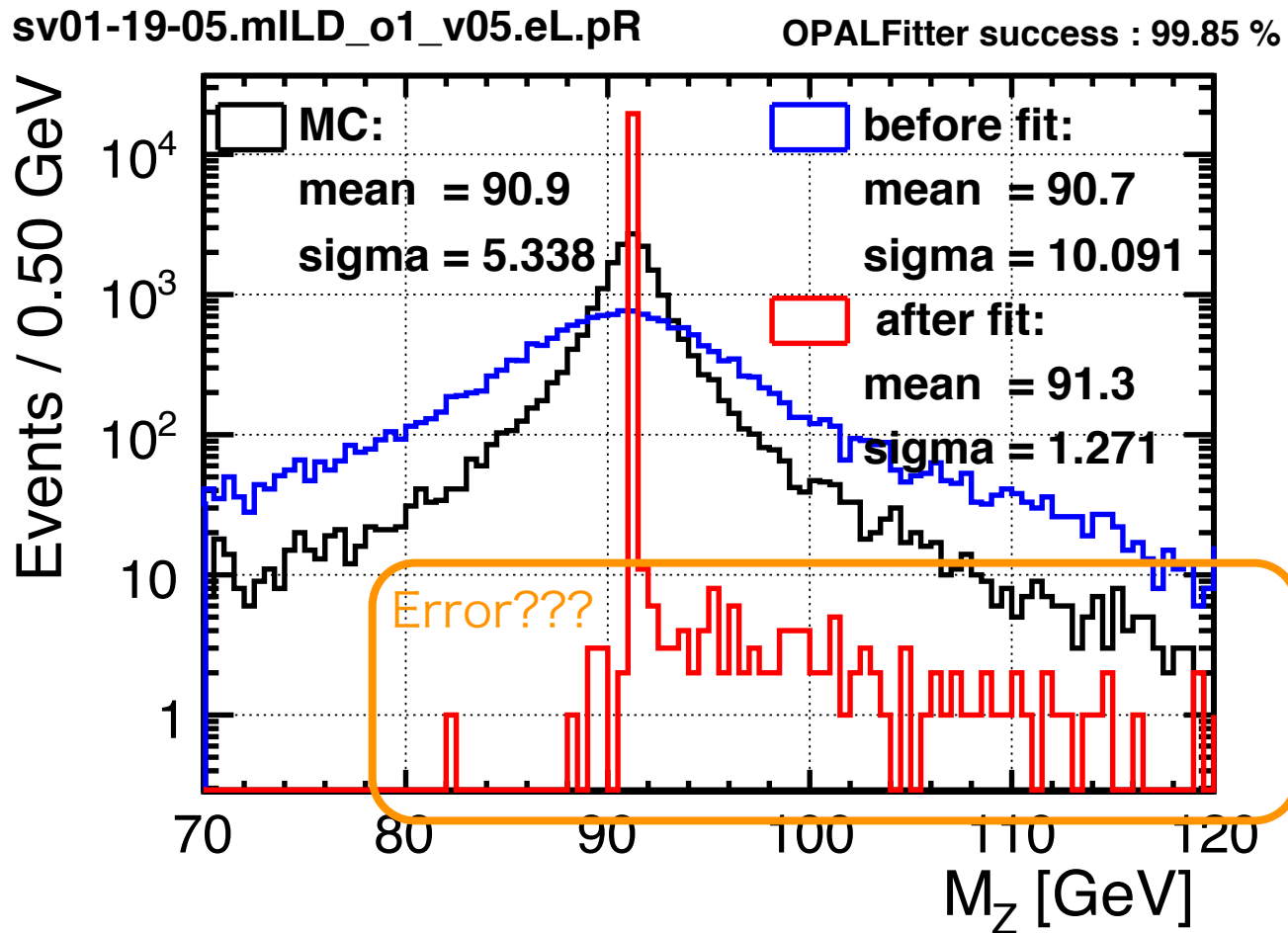
$$M_{rec} = \sqrt{(\sqrt{s} - E_Z)^2 - |\vec{p}_Z|^2}$$

$$\delta M_{rec} = \frac{M_{rec}^{result} - M_{rec}^{mc}}{M_{rec}^{mc}}$$

improve recoil mass resolution ~20%



Problems : Z mass distribution

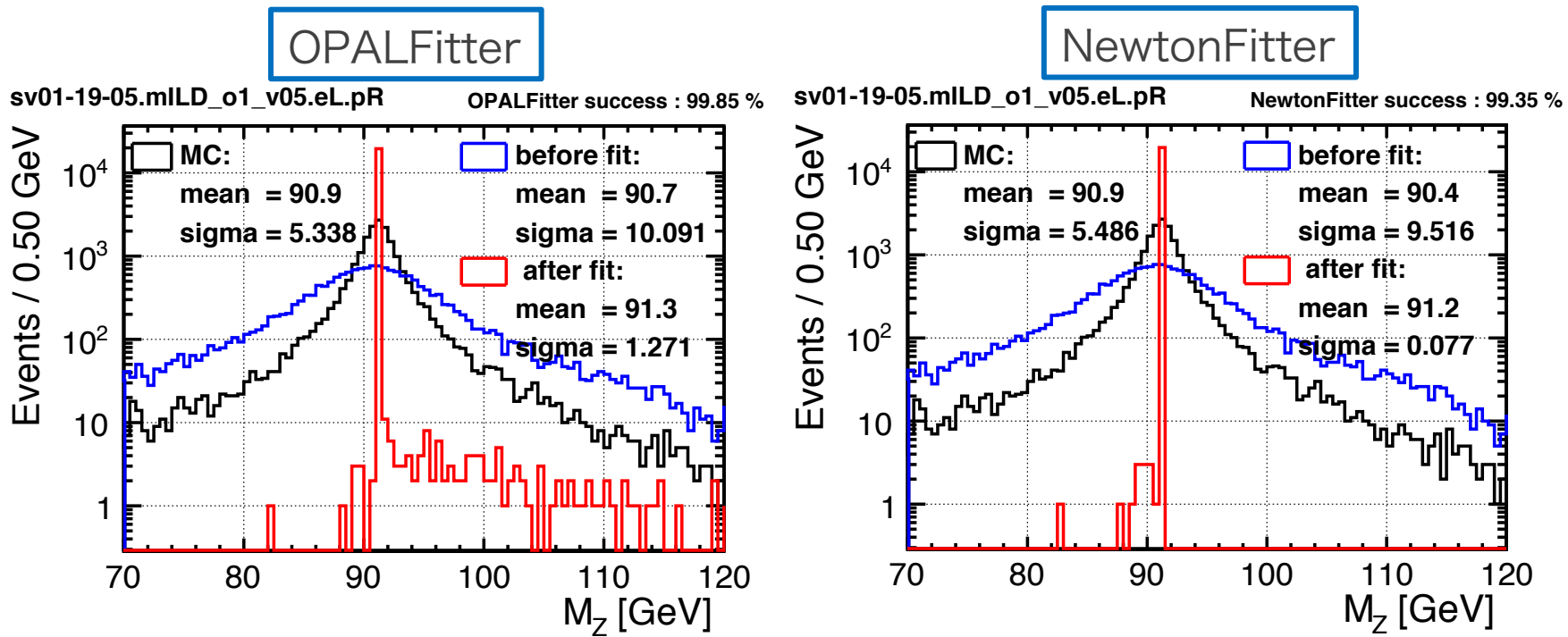


kinematic fit

the Cause:

Approximate calculation of constraint in OPALFitter

$$f_i(\vec{\eta}^{\nu+1}, \vec{\xi}^{\nu+1}) = f_i(\vec{\eta}^\nu, \vec{\xi}^\nu) + \left. \frac{\partial f_i}{\partial \eta_j} \right|_{\eta_j=\eta_j^\nu} (\eta_j^{\nu+1} - \eta_j^\nu) + \left. \frac{\partial f_i}{\partial \xi_k} \right|_{\xi_k=\xi_k^\nu} (\xi_k^{\nu+1} - \xi_k^\nu)$$



Search for BSM using $H \rightarrow$ invisible

Higgs \rightarrow invisible Analysis

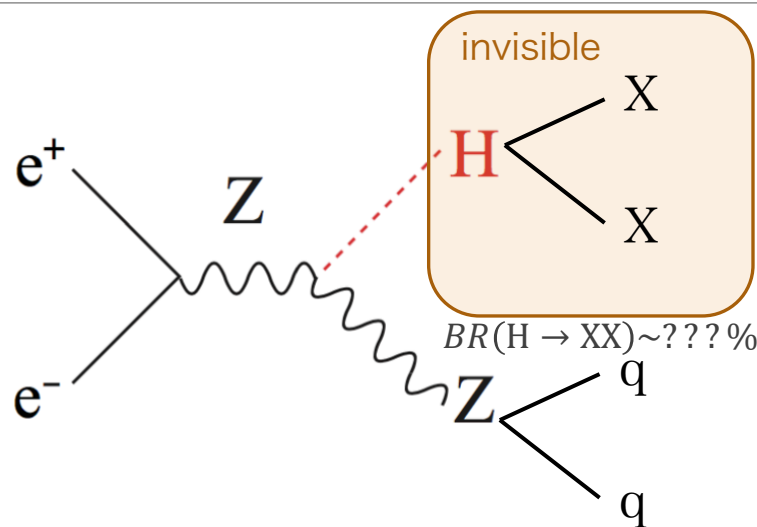
● Simulation set up

- Generator: WHIZARD 1.95
 - Samples: DBD sample + Dirac sample ($e^+e^- \rightarrow qqH, H \rightarrow ZZ^* \rightarrow 4\nu$)
 - Detector: ILD full simulation (ILD_o1_v05)
 - $\sqrt{s} = 250 \text{ GeV}$, $\int L dt = 250 \text{ fb}^{-1}$, $(P_{e^-}, P_{e^+}) = (-0.8, +0.3), (+0.8, -0.3)$
“Left” “Right”

● Flow of analysis

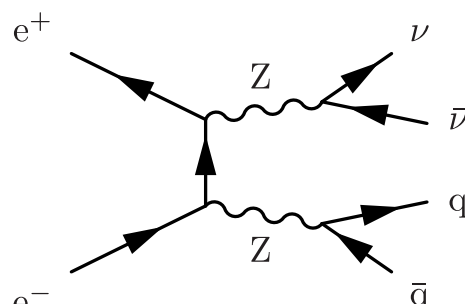
1. Reconstruction : “PandoraPFA”
 - Isolated lepton tagging
 2. 2 jet clustering : “Durham algorithm”
 - Forced 2 jet clustering
 3. **kinematic fit**
 4. Event selection
 - Assume $\text{BR}(H \rightarrow \text{invisible}) = 10\%$
 5. Estimate upper limit of BR.
 - Template method: $\text{BR}(H \rightarrow \text{invisible}) = [1, 2, \dots, 10\%]$

Higgs \rightarrow invisible Signal

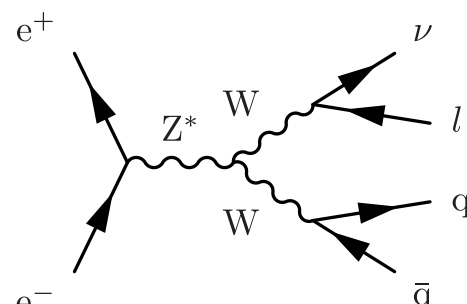


- ✓ 2 jet & missing E
- ✓ $M_{qq} \approx M_Z$: $BR(Z \rightarrow qq) \sim 70\%$
- ✓ $M_{recoil} \approx M_{Higgs}$
- ✓ s channel process

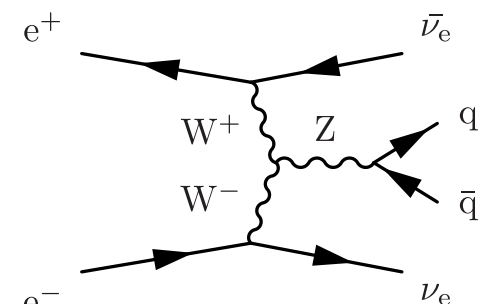
Main background



ZZ semi-leptonic



WW semi-leptonic



$\nu\nu Z$ semi-leptonic

Higgs→invisible

Cut table $(P_{e^-}, P_{e^+}) = (-0.8, +0.3)$

cut condition	S/ $\sqrt{S+B}$	signal	all bkg	ZZ	WW	$\nu\nu Z$	other bkg
No Cut	0.84	5255	3.93×10^7	214211	2748230	67952	3.63×10^7
$N_{lep} = 0$	1.00	5249	2.74×10^7	165399	1276030	67853	2.59×10^7
Pre-Cut	7.54	5026	439363	35027	69535	33852	300949
$N_{pfo} > 15 \& N_{charged} > 6$	9.66	4947	256873	34332	67457	33236	121848
$p_{T,jj} \in (20, 80)\text{GeV}$	12.48	4688	136149	30207	56149	29166	20627
$M_{jj} \in (80, 100)\text{GeV}$	13.50	3919	80266	23533	29210	23675	3848
$ \cos\theta_{jj} < 0.9$	13.94	3768	69199	20457	24817	21246	2679

w/o kinematic fit

cut condition	S/ $\sqrt{S+B}$	signal	all bkg	ZZ	WW	$\nu\nu Z$	other bkg
common part	13.94	3768	69199	20457	24817	21246	2679
$M_{recoil} \in (100, 160)\text{GeV}$	13.95	3765	69002	20438	24748	21174	2642
BDT > -0.0718	15.54	3388	44086	12604	14941	14676	1865

w/ kinematic fit

cut condition	S/ $\sqrt{S+B}$	signal	all bkg	ZZ	WW	$\nu\nu Z$	other bkg
common part	13.94	3768	69199	20457	24817	21246	2679
$M_{recoil} \in (100, 160)\text{GeV}$	15.10	3766	58404	15873	21289	18665	2577
BDT > -0.0867	16.26	3425	40893	11086	14030	13903	1874

Higgs→invisible

Cut table $(P_{e^-}, P_{e^+}) = (+0.8, -0.3)$

cut condition	S/ $\sqrt{S+B}$	signal	all bkg	ZZ	WW	$\nu\nu Z$	other bkg
No Cut	0.76	3549	2.16×10^7	116792	189591	23127	2.13×10^7
$N_{lep} = 0$	0.95	3545	1.39×10^7	89111	88065	23092	1.37×10^7
Pre-Cut	7.33	3391	210605	16373	4918	8970	180344
$N_{pfo} > 15 \& N_{charged} > 6$	10.03	3331	106837	16028	4773	8786	77250
$p_{T_{jj}} \in (20, 80)\text{GeV}$	15.59	3144	37369	14018	4022	7793	11536
$M_{jj} \in (80, 100)\text{GeV}$	17.17	2632	20815	10828	2087	6121	1779
$ \cos\theta_{jj} < 0.9$	17.81	2535	17670	9387	1806	5373	1104

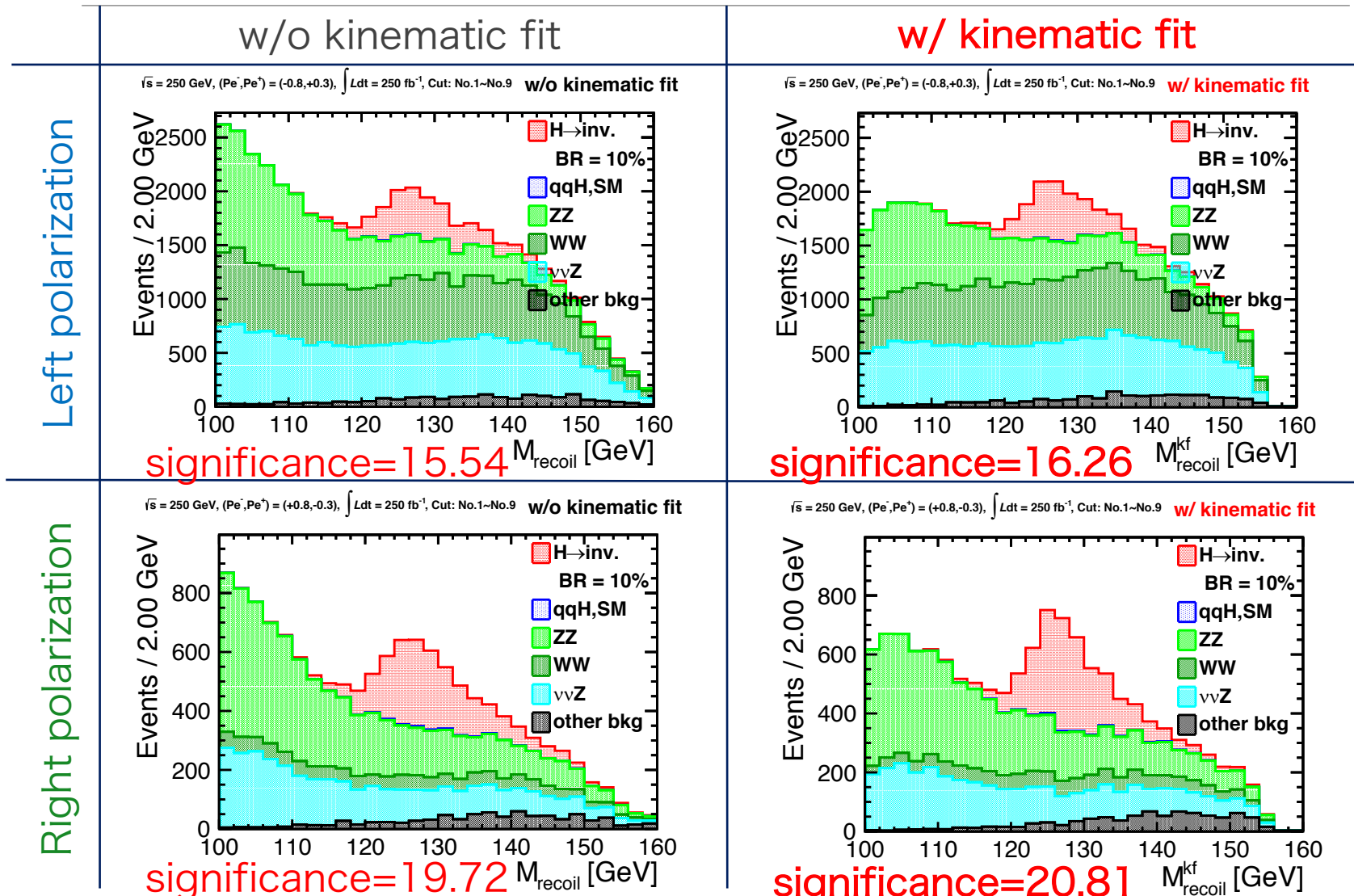
w/o kinematic fit

cut condition	S/ $\sqrt{S+B}$	signal	all bkg	ZZ	WW	$\nu\nu Z$	other bkg
common part	17.81	2535	17670	9387	1806	5373	1104
$M_{recoil} \in (100, 160)\text{GeV}$	17.83	2532	17598	9376	1800	5366	1056
BDT > -0.0840	19.72	2298	11231	5800	1170	3463	798

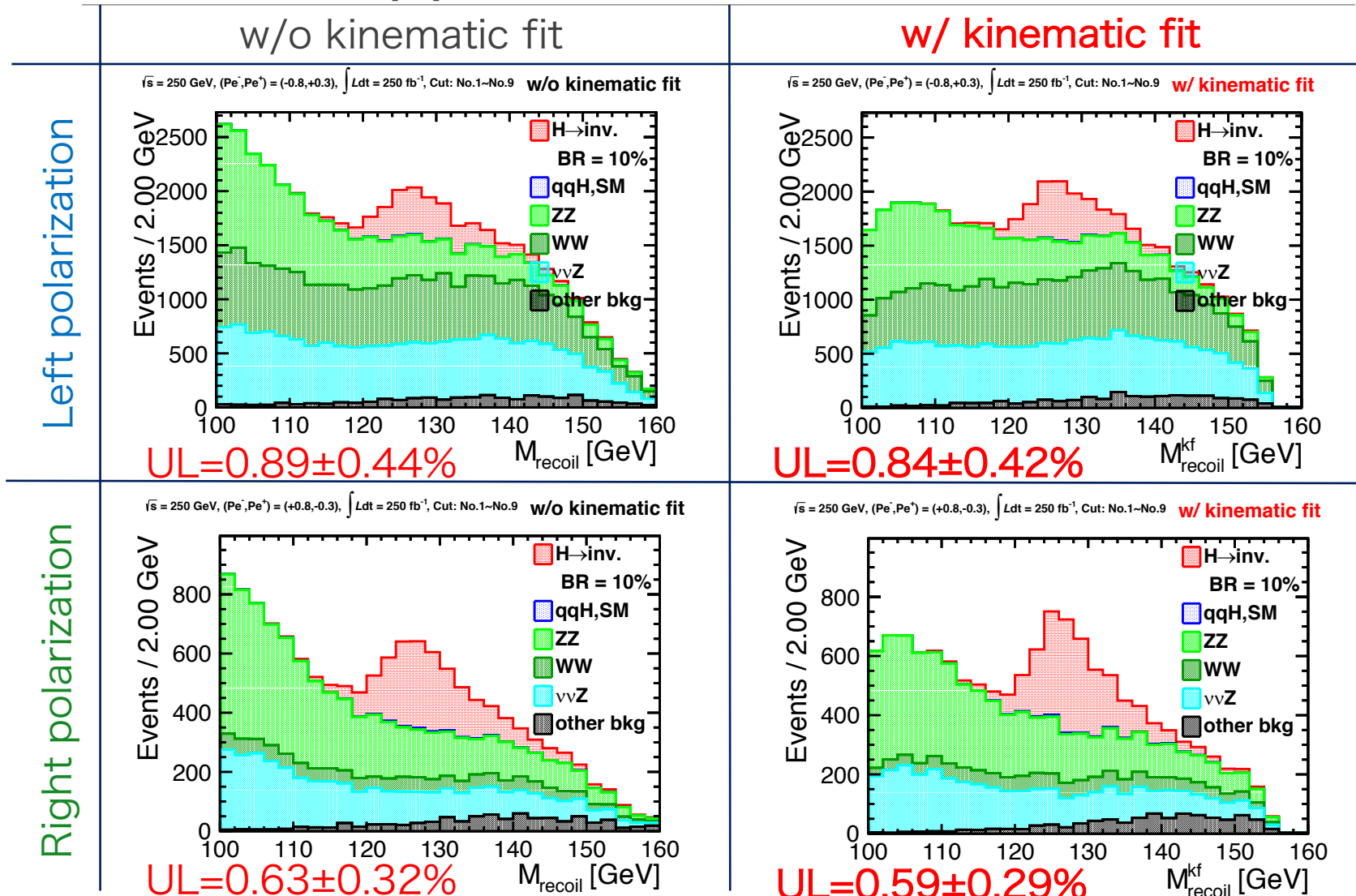
w/ kinematic fit

cut condition	S/ $\sqrt{S+B}$	signal	all bkg	ZZ	WW	$\nu\nu Z$	other bkg
common part	17.81	2535	17670	9387	1806	5373	1104
$M_{recoil} \in (100, 160)\text{GeV}$	19.61	2533	14104	7196	1549	4274	1085
BDT > -0.1162	20.81	2395	10806	5431	1187	3318	870

Result : Recoil mass distribution



Result : Upper limit of BR (95% CL)



Summary

Evaluate jet energy resolution

ILD model : ILD_I(s)5_v02

- jet energy & $\cos \theta$ dependence
- evaluate jet angle resolution also
- apply to kinematic fit

kinematic fit

fit variables : $E_{j1}, \theta_{j1}, \phi_{j1}, E_{j2}, \theta_{j2}, \phi_{j2}$

constraint : $m_{jj} = m_Z = 91.2 \text{ GeV}$

MarlinKinfit : OPALFitter

apply jet resolution

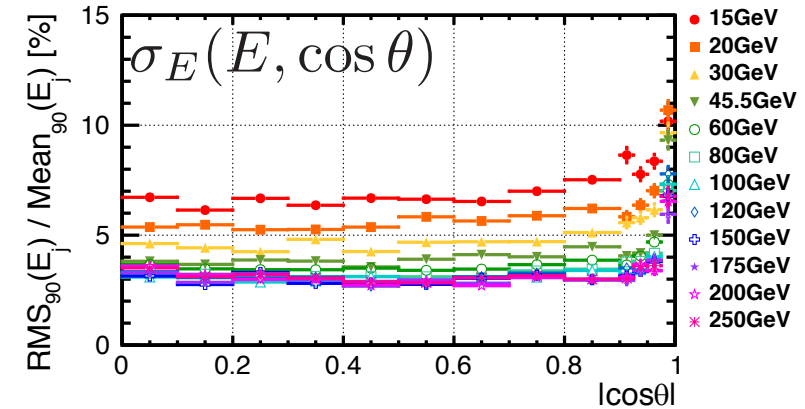
Higgs \rightarrow invisible

Estimate upper limit of $\text{BR}(H \rightarrow \text{inv.})$

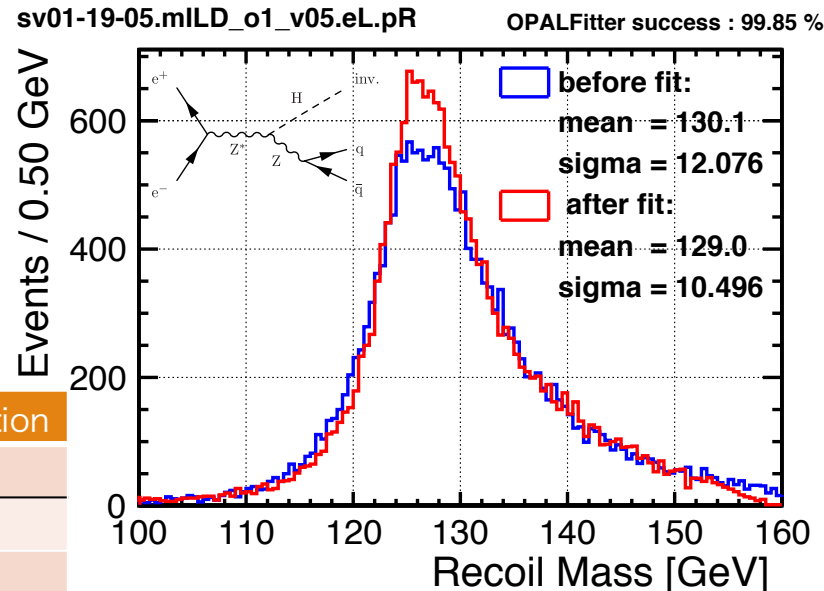
Check effect by kinematic fit

UL of BR [%] (95%CL)	Left polarization	Right polarization
Previous study	0.95	0.69
w/o kinematic fit	0.89 ± 0.44	0.63 ± 0.32
w/ kinematic fit	0.84 ± 0.42	0.59 ± 0.29

sv01-19-05.mILD_I5_o1_v02_nobg



sv01-19-05.mILD_o1_v05.eL.pR



今後の課題

ジェットエネルギー分解能評価

- エンドキャップ部分のより精細な評価 ← 統計量の増加
- cジェット、bジェット評価の追加
- ジェットクラスタリングを用いた評価： $E_{j1} \neq E_{j2}$
- ジェット質量(または運動量)依存性の追加

kinematic fit

- フィッティング精度の改善：分解能をスケールする
- soft constraintの実装：Zボソンの自然幅を考慮
- 他の物理過程への応用

Higgs→invisible崩壊分岐比の上限推定

- 反跳質量以外のフィット後の変数を事象選別に使用
- 推定に用いる反跳質量領域の最適化
- より高度な手法を用いて上限評価
ex.) profile likelihood ratio

backup

The Mathematics of the NewtonFitter

N parameters a_i , $i = 1 \dots N$ Measured values \vec{y} , covariance matrix V

K constraint functions $\vec{f}(\vec{a})$

The total χ^2 : $\chi_T^2(\vec{a}, \vec{\lambda}) = \chi^2(\vec{a}, \vec{y}) + \vec{\lambda}^T \cdot \vec{f}(\vec{a})$.

Seek stationary point, where all derivatives vanish:

$$\begin{aligned}\nabla_a \chi_T^2 &= \nabla_a \chi^2 + \vec{\lambda}^T \cdot \nabla_a \vec{f}(\vec{a}) = \vec{0}, & (N \text{ equations}) \\ \nabla_{\lambda} \chi_T^2 &= \vec{f}(\vec{a}) = \vec{0}, & (K \text{ equations})\end{aligned}\quad \left(\begin{array}{c} 0 \\ 0 \end{array} \right) = \left(\begin{array}{c} \frac{\partial \chi_T^2}{\partial a_i} \\ \frac{\partial \chi_T^2}{\partial \lambda_k} \end{array} \right) = \left(\begin{array}{c} \frac{\partial \chi^2}{\partial a_i} + \sum_k \lambda_k \cdot \frac{\partial f_k}{\partial a_i} \\ f_k \end{array} \right)$$

Newton-Raphson iterative method to solve $y(x)=0$:

$$x^{\nu+1} = x^\nu - \frac{y(x^\nu)}{y'(x^\nu)} \Rightarrow \text{solve } y'(x^\nu) \cdot (x^\nu - x^{\nu+1}) = y(x^\nu)$$

Here: Solve this system of equations in each step:

$$\left(\begin{array}{ccc|ccc} \frac{\partial^2 \chi^2}{\partial a_1 \partial a_1} + \lambda_k \cdot \frac{\partial^2 f_k}{\partial a_1 \partial a_1} & \dots & \frac{\partial^2 \chi^2}{\partial a_1 \partial a_N} + \lambda_k \cdot \frac{\partial^2 f_k}{\partial a_1 \partial a_N} & \frac{\partial f_1}{\partial a_1} & \dots & \frac{\partial f_K}{\partial a_1} \\ \dots & & \dots & \dots & \dots & \dots \\ \frac{\partial^2 \chi^2}{\partial a_N \partial a_1} + \lambda_k \cdot \frac{\partial^2 f_k}{\partial a_N \partial a_1} & \dots & \frac{\partial^2 \chi^2}{\partial a_N \partial a_N} + \lambda_k \cdot \frac{\partial^2 f_k}{\partial a_N \partial a_N} & \frac{\partial f_1}{\partial a_N} & \dots & \frac{\partial f_K}{\partial a_N} \\ \hline \frac{\partial f_1}{\partial a_1} & \dots & \frac{\partial f_1}{\partial a_N} & 0 & \dots & 0 \\ \dots & & \dots & \dots & \dots & \dots \\ \frac{\partial f_K}{\partial a_1} & \dots & \frac{\partial f_K}{\partial a_N} & 0 & \dots & 0 \end{array} \right) \cdot \left(\begin{array}{c} a_1^\nu - a_1^{\nu+1} \\ \dots \\ a_N^\nu - a_N^{\nu+1} \\ \hline \lambda_1^\nu - \lambda_1^{\nu+1} \\ \dots \\ \lambda_K^\nu - \lambda_K^{\nu+1} \end{array} \right) = \left(\begin{array}{c} \frac{\partial \chi^2}{\partial a_1} + \lambda_k^\nu \cdot \frac{\partial f_k}{\partial a_1} \\ \dots \\ \frac{\partial \chi^2}{\partial a_N} + \lambda_k^\nu \cdot \frac{\partial f_k}{\partial a_N} \\ \hline f_1 \\ \dots \\ f_K \end{array} \right)$$

List of envelope parameters for ILD_I5_v02						
detector	inner radius	outer radius	half length min z, max z	additional parameters		
VXD	15.0	101.0	177.6	VXD_cone_min_z VXD_cone_max_z VXD_inner_radius_1	80.0 150.0 25.1	
FTD	37.0	309.0	2350.0	FTD_outer_radius_1 FTD_outer_radius_2 FTD_min_z_0 FTD_min_z_1 FTD_min_z_2 FTD_cone_min_z FTD_cone_radius	152.8 299.7 177.7 368.2 644.2 230.0 192.0	
SIT	152.9	324.6	644.1	SIT_outer_radius_1 SIT_half_length_1	299.8 368.1	
TPC	329.0	1769.8	2350.0			
SET	1769.9	1804.3	2350.0			
Ecal	1804.8	2028.0	2350.0	Ecal_Hcal_symmetry Ecal_symmetry	8 8	
EcalEndcap	400.0	2095.84	2411.8, 2635.0	EcalEndcap_symmetry	8	
EcalEndcapRing	250.0	390.0	2411.8, 2635.0			
Hcal	2058.0	3395.5	2350.0	Hcal_inner_symmetry	8	
HcalEndcap	350.0	3225.5	2650.0, 3937.0			
HcalEndcapRing	2145.84	2980.0	2411.8, 2635.0	HcalEndcapRing_symmetry	8	
Coil	3425.0	4175.0	3872.0			
Yoke	4475.0	7776.0	4047.0	Yoke_symmetry	12	
YokeEndcap	300.0	7776.0	4072.0, 7373.0	YokeEndcap_symmetry	12	
YokeEndcapPlug	300.0	3395.54	3937.2, 4072.0	YokeEndcapPlug_symmetry	12	
BeamCal	17.8	140.0	3115.0, 3315.0	BeamCal_thickness	200.0	
LHCal	130.0	315.0	2680.0, 3160.0	LHCal_thickness	480.0	
LumiCal	80.0	202.1	2411.8, 2540.5	LumiCal_thickness	128.7	

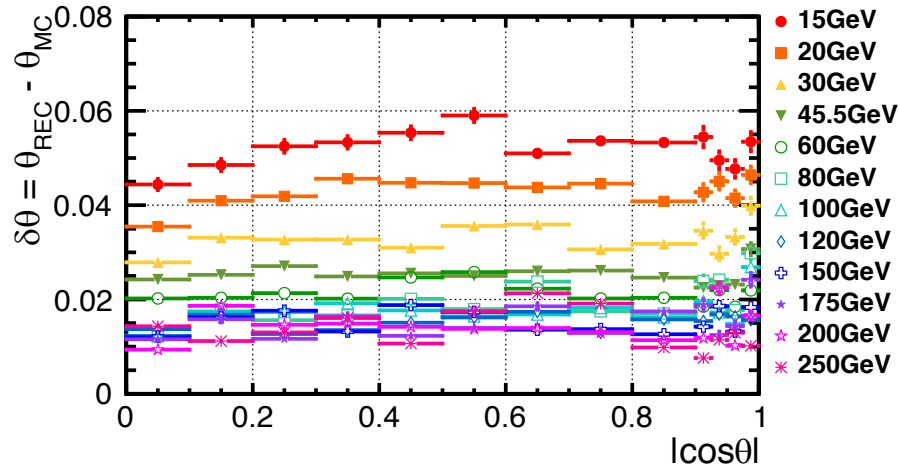
List of envelope parameters for ILD_s5_v02						
detector	inner radius	outer radius	half length min z, max z	additional parameters		
VXD	15.0	101.0	177.6	VXD_cone_min_z VXD_cone_max_z VXD_inner_radius_1	80.0 150.0 25.1	
FTD	37.0	309.0	2350.0	FTD_outer_radius_1 FTD_outer_radius_2 FTD_min_z_0 FTD_min_z_1 FTD_min_z_2 FTD_cone_min_z FTD_cone_radius	152.8 299.7 177.7 368.2 644.2 230.0 192.0	
SIT	152.9	324.61	644.1	SIT_outer_radius_1 SIT_half_length_1	299.8 368.1	
TPC	329.0	1426.8	2350.0			
SET	1426.9	1461.3	2350.0			
Ecal	1461.8	1685.0	2350.0	Ecal_Hcal_symmetry Ecal_symmetry	8 8	
EcalEndcap	400.0	1717.92	2411.8, 2635.0	EcalEndcap_symmetry	8	
EcalEndcapRing	250.0	390.0	2411.8, 2635.0			
Hcal	1715.0	3045.83	2350.0	Hcal_inner_symmetry	8	
HcalEndcap	350.0	2875.83	2650.0, 3937.0			
HcalEndcapRing	1767.92	2656.92	2411.8, 2635.0	HcalEndcapRing_symmetry	8	
Coil	3075.33	3825.33	3872.0			
Yoke	4125.33	7426.33	4047.0	Yoke_symmetry	12	
YokeEndcap	300.0	7426.33	4072.0, 7373.0	YokeEndcap_symmetry	12	
YokeEndcapPlug	300.0	3045.83	3937.2, 4072.0	YokeEndcapPlug_symmetry	12	
BeamCal	17.8	140.0	3115.0, 3315.024	BeamCal_thickness	220.03	
LHCal	130.0	315.0	2680.0, 3160.0	LHCal_thickness	480.0	
LumiCal	80.0	202.09	2411.8, 2540.5	LumiCal_thickness	128.7	

Angular resolution

polar angle

$$\delta\theta = RMS_{90}(\theta_{rec} - \theta_{mc})$$

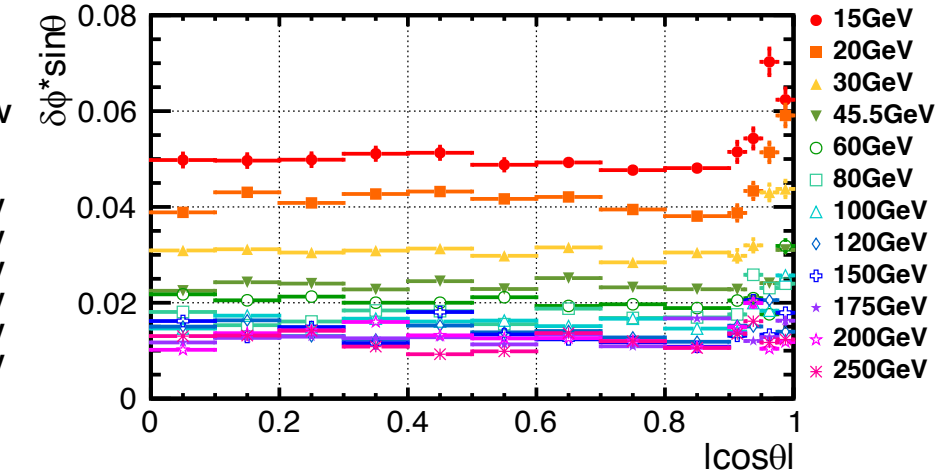
sv01-19-05.mILD_I5_o1_v02_nobg



azimuth angle

$$\delta\phi * sin\theta = RMS_{90}\{(\phi_{rec} - \phi_{mc})sin\theta\}$$

sv01-19-05.mILD_I5_o1_v02_nobg



For evaluation of angular resolution,
use jet clustering.

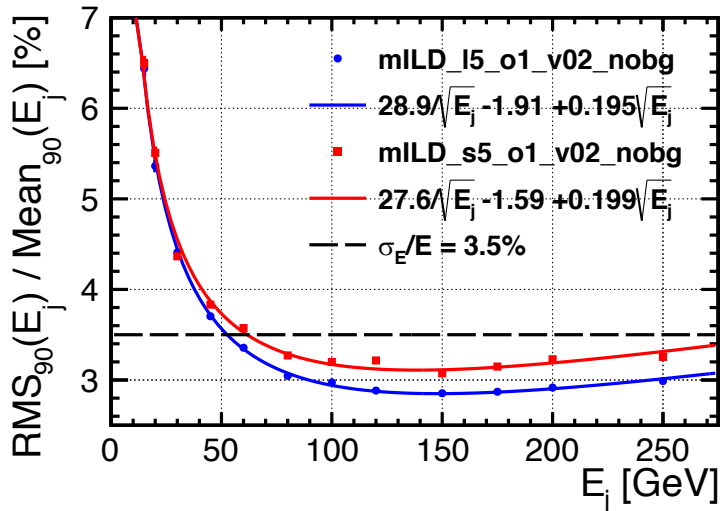
Durham algorithm

$$y_{ij} = \frac{2\min(E_i^2, E_j^2)(1 - \cos\theta_{ij})}{Q^2}$$

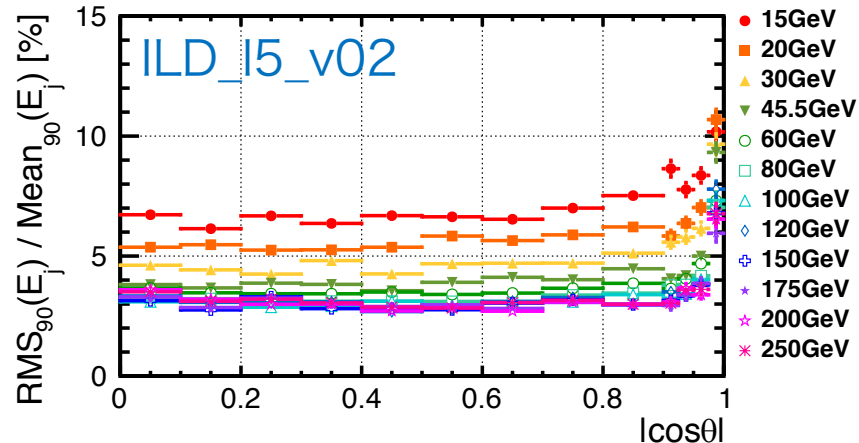
apply this result to kinematic fit

Compare with

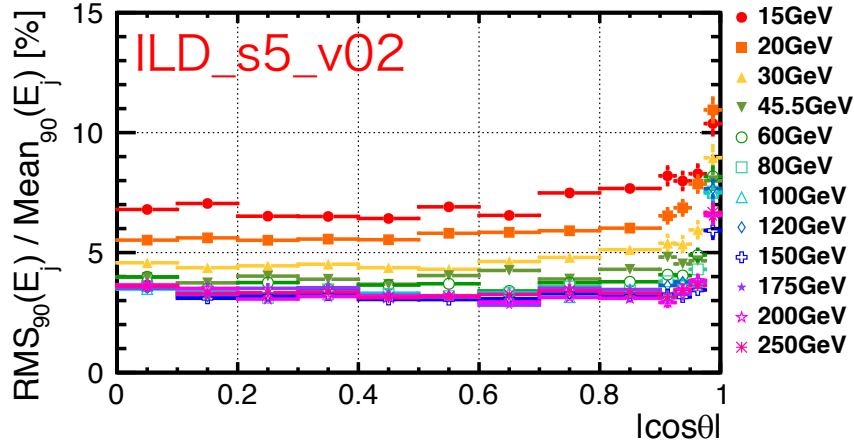
sv01-19-05 $|\cos\theta| < 0.7$



sv01-19-05.mILD_I5_o1_v02_nobg



sv01-19-05.mILD_s5_o1_v02_nobg



エネルギー分解能の定義

$$\frac{\sigma_{E_j}}{E_j} = \frac{\text{RMS}_{90}(E_j)}{\text{mean}_{90}(E_j)} = \sqrt{2} \frac{\text{RMS}_{90}(E_{jj})}{\text{mean}_{90}(E_{jj})}$$

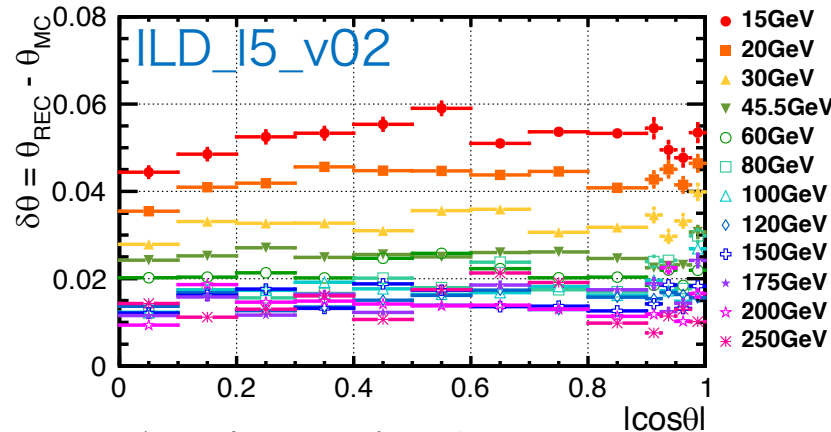
RMS₉₀

ヒストグラム内の90%の事象が含まれる
最小の領域における標準偏差を用いる

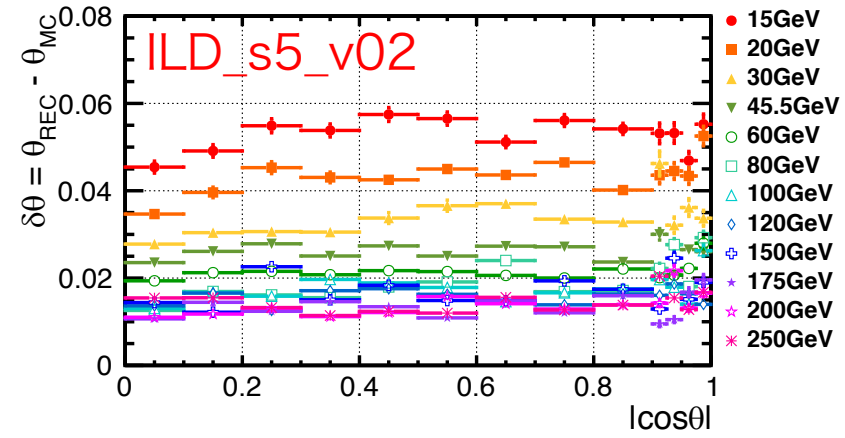
極角分解能

$$\delta\theta = RMS_{90}(\theta_{rec} - \theta_{mc})$$

sv01-19-05.mILD_I5_o1_v02_nobg

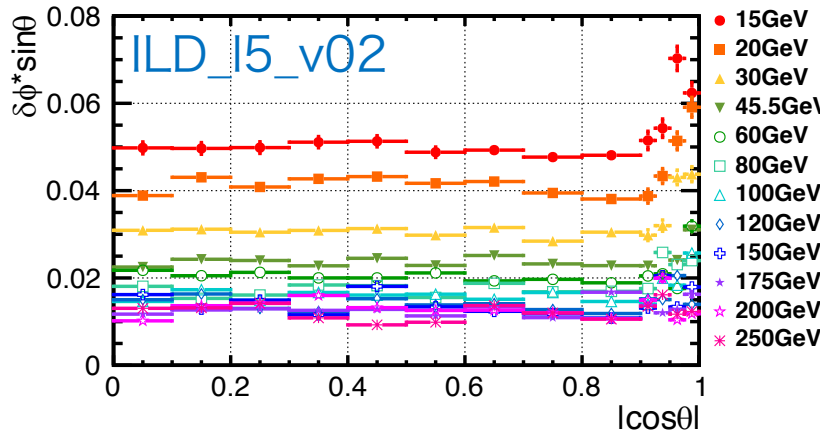


sv01-19-05.mILD_s5_o1_v02_nobg

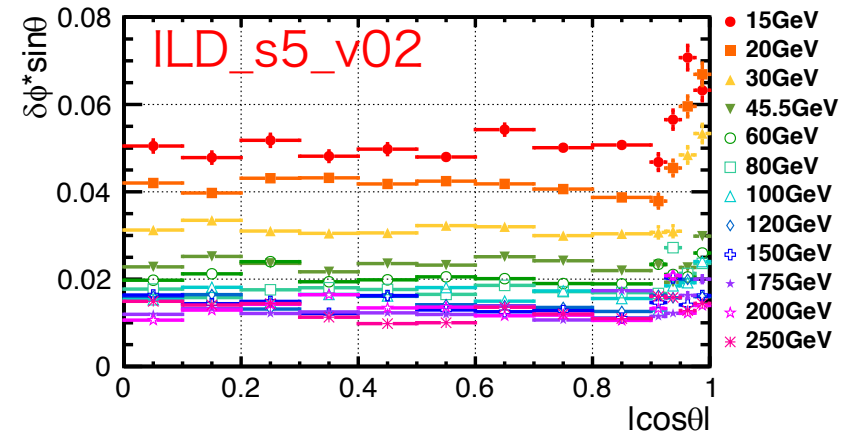


方位角分解能 $\delta\phi * sin\theta = RMS_{90}\{(\phi_{rec} - \phi_{mc})sin\theta\}$

sv01-19-05.mILD_I5_o1_v02_nobg



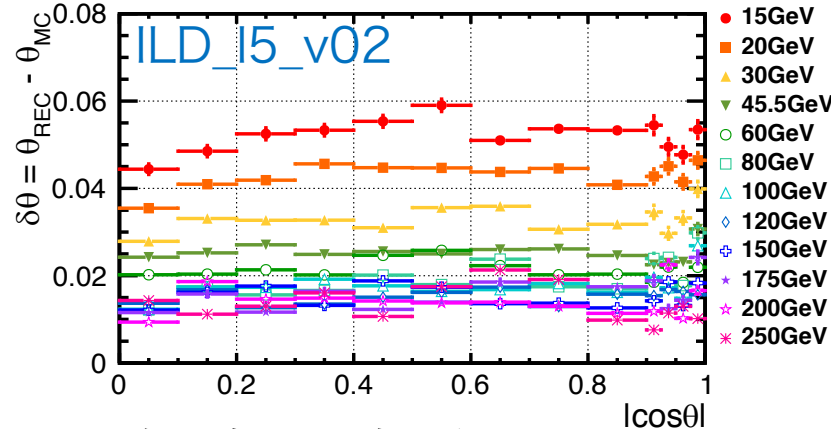
sv01-19-05.mILD_s5_o1_v02_nobg



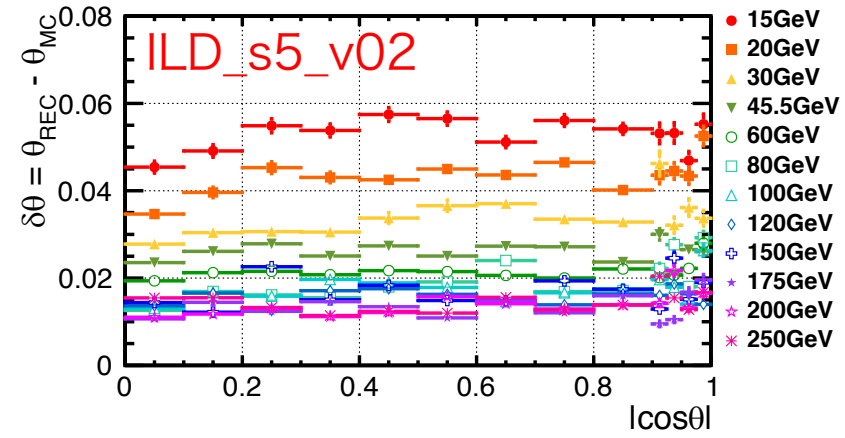
極角分解能

$$\delta\theta = RMS_{90}(\theta_{rec} - \theta_{mc})$$

sv01-19-05.mILD_I5_o1_v02_nobg



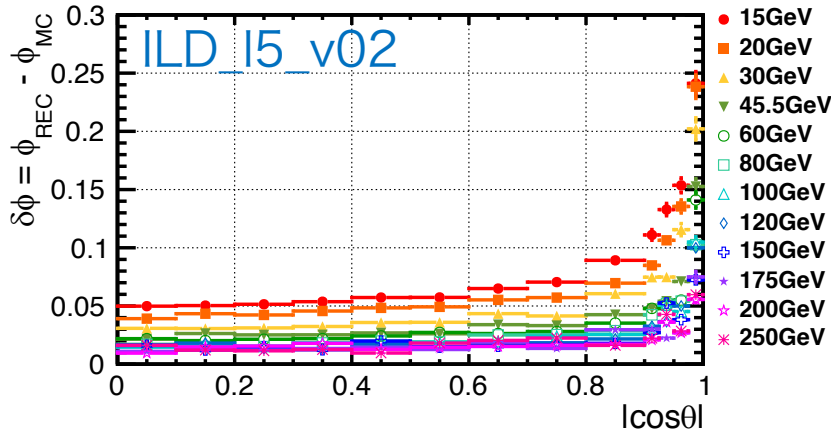
sv01-19-05.mILD_s5_o1_v02_nobg



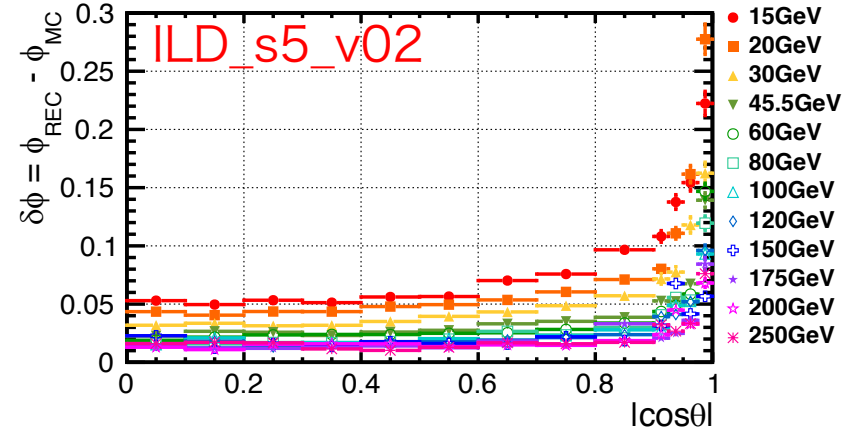
方位角分解能

$$\delta\phi = RMS_{90}(\phi_{rec} - \phi_{mc})$$

sv01-19-05.mILD_I5_o1_v02_nobg



sv01-19-05.mILD_s5_o1_v02_nobg



Event Selection

1. isolated lepton veto
2. loose restriction
[transverse di-jet momentum, di-jet invariant mass, recoil mass from di-jet]
3. number of PFOs and charged tracks: N_{pfo} , N_{track}
4. di-jet (Z) pt: Pt_Z
5. di-jet mass: M_Z
6. di-jet polar angle: θ_Z
7. recoil mass: M_{recoil}
8. multi-variate analysis: Boosted Decision Tree(BDT) method

生成断面積とモンテカルロサンプル

サンプル名	生成断面積 [fb ⁻¹]		生成事象数	
	左完全偏極	右完全偏極	左完全偏極	右完全偏極
qqH, H → inv.(BR = 10%)	34.6	22.2	19701	19900
qqH (SM)	346.0	222.0	346336	222351
ZZ semi-leptonic	1422.1	713.5	356461	178635
WW semi-leptonic	18781.0	172.7	1919148	43501
$\nu\nu Z$ semi-leptonic	456.8	130.8	114516	32998
other bkg	223851	114716	17312470	

左完全偏極 : $(P_{e^-}, P_{e^+}) = (-1.0, +1, 0)$

右完全偏極 : $(P_{e^-}, P_{e^+}) = (+1.0, -1, 0)$

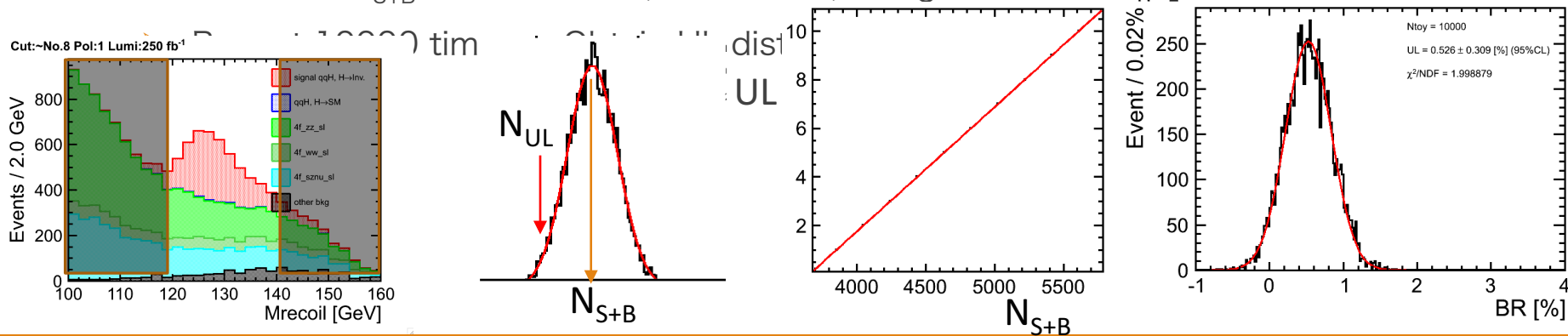
How to set UL [Statistical method]

● Template

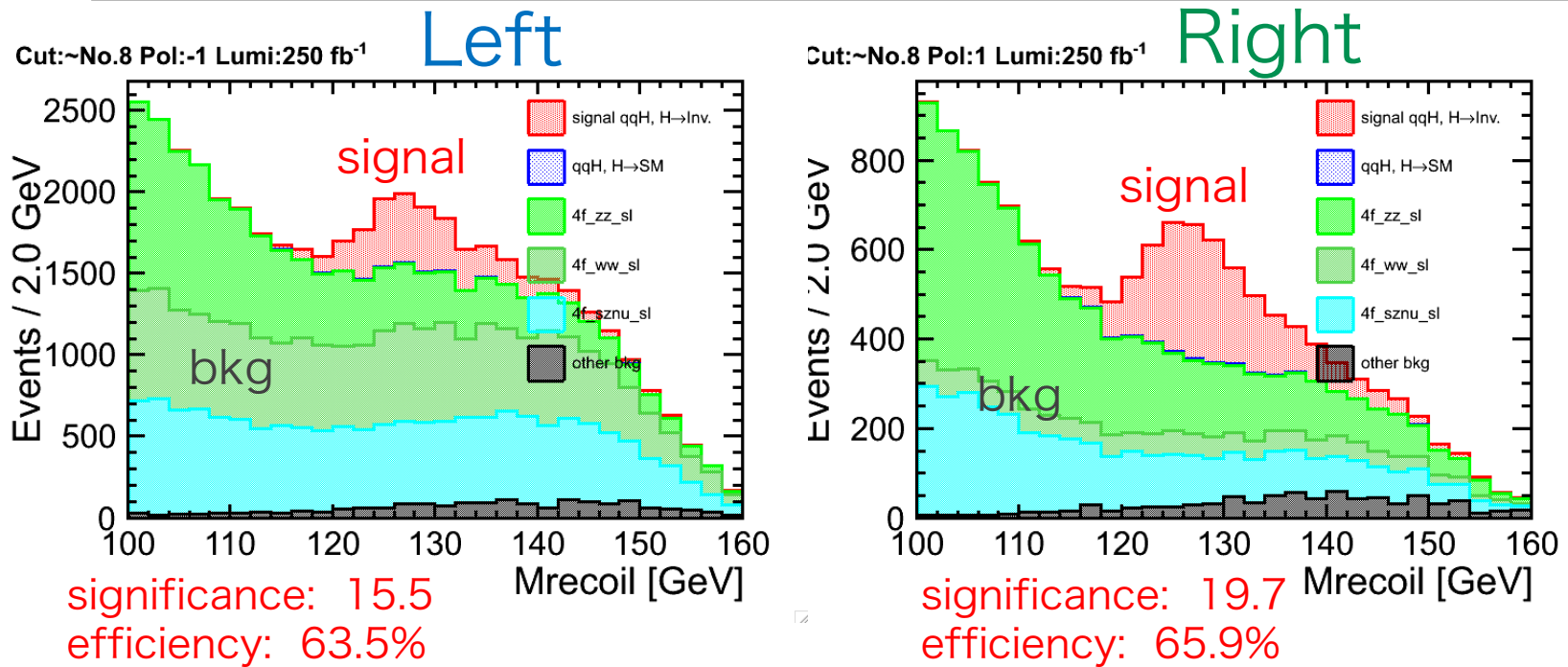
- Assume $\text{BR}(\text{H} \rightarrow \text{invisible}) = [1, 2, \dots, 10]\%$ -> Event selection
- Get # of events (N_{S+B}) in window range ($M_{\text{recoil}} \in [120, 140]$ GeV)
- Generate Poisson distribution of N_{S+B} -> Get 95% CL limit (N_{UL})
- Repeat for each $\text{BR}(\text{H} \rightarrow \text{invisible}) = [1, 2, \dots, 10]\%$ -> Get calibration line between N_{UL} and UL

● Toy MC

- Fit template bkg -> Generate pseudo experiment by fluctuated bkg function
- Get # of events (N_{S+B}) in window range ($M_{\text{recoil}} \in [120, 140]$ GeV)
- Translate N_{S+B} into UL of $\text{BR}(\text{H} \rightarrow \text{invisible})$ using calibration line



Result of Mrec dist. [Ecm = 250 GeV, 250 fb⁻¹, BR(H→inv.)=10%]



MVA input variables	
di-jet inv. mass	one jet polar angle
di-jet polar angle	another jet polar angle

TMVA v-4.2.0

No.	Cut	No.	Cut
1	Isolated lepton veto	5	80 < di-jet invariant mass < 100
2	Loose Cut (Pt _z , M _z , M _{recoil})	6	di-jet polar angle < 0.9
3	#pfo > 15 & #all_track > 6 & # track_in_one_jet > 1	7	100 < recoil mass < 160
4	20 GeV < di-jet Pt < 80 GeV	8	BDT cut